

## ON ANALYSIS OF FAILURE EMANATING FROM A NOTCH

G. PLUVINAGE

Université de Lorraine, École Nationale d'ingénieurs de Metz, France;  
Fiabilité Mécanique, Conseils, Lorraine, France

Notch-like defect assessment is not done using classical fracture mechanics (mechanics of cracks). In order to prevent over-conservatism, notch fracture mechanics concepts such as notch stress intensity factor or notch energy integral  $J_p$  are generally used for that. A local stress criterion, named volumetric method, defines effective stress. It is used for more advanced assessment when introducing geometry and constraint effects. These effects are taken into account for notch fracture toughness and constraint modified notch failure assessment diagram.

**Keywords:** notch, fracture mechanics, failure assessment diagram.

**Failure emanating from notches.** Failure is governed by the critical conjunction of three elements: defect, loading and fracture resistance. A large variety of defects can promote failure. Crack, among them, is the most severe as considered ideally with an infinite acuity. Notches are considered as less severe with a finite acuity. Notch severity depends strongly on the notch acuity as the inverse of the notch radius. Notches are responsible for a large number of component failures. As an example, the failure emanating from a column with a square thread of a friction screw press is shown in Fig. 1. The thread was not rounded off in the roots and the flanks exhibited striations, both of these factors increased the notch effect. Striations are particularly numerous at point A (Fig. 1), which also denotes the point of fatigue initiation.

In this paper special attention is paid to notches which appear at oil or gas pipe surfaces. These notches or scratches are generally created by excavator when the works are carried out on the nearby pipes. These incidents, called external interferences, are considered as responsible for more than 50% of pipe failure in Western Europe [1].

Prediction of failure emanating from a notch cannot be done using classical fracture mechanics, which considers the failure promoting defect as a crack-like one. Therefore, this approach is too much conservative. Past methods are based on the stress concentration factor which considers that failure is initiated at the notch root, which is only the case of brittle fracture and with a



Fig. 1. Failure emanating from a column with a square thread of a friction screw press (diameter of the column is 97.5 mm; outer and internal diameter of the square thread equals 96 mm and 88.1 mm, respectively).

particular approach of failure mechanism. It is considered that the fracture driving force is concentrated at one point and therefore its density is infinite. To overcome this difficulty, notch fracture mechanics (NFM) has been developed [2]. Notch acuity is taken into account through notch tip stress distribution and different failure criteria (local or global). It has been admitted since Neuber [3] or Novozilov [4] that fracture needs a process volume in which the necessarily available energy is stored. For the sake of simplicity, this volume is considered as cylindrical with a height equal to the thickness of the component and a radius called the effective distance. Inside this volume, the stress distribution is averaged by different methods. This averaged stress is denoted as an effective stress.

In this paper, starting from stress distribution at the notch tip, the effective distance and the effective stress are described through a volumetric method (VM) [5] and combined into notch stress intensity factor (NSIF). These fracture parameters are used to describe the influence of notch acuity on fracture toughness. Its increase, with the increase of the notch radius, is taken into account in defect assessment in order to reduce conservatism. This can be done using a notch failure assessment diagram (NFAD).

**On local fracture criterion for a notch.** Failure assessment can be done by several fracture criteria (more than 30!). These criteria can be classified as energy, stress, and strain-based. Each of these categories can be divided into a local and a global one. They provide a relationship between defect size, loading, and fracture toughness i.e. a three parameters failure approach. Additionally, failure criteria based on two parameters have been proposed in a failure assessment diagram (FAD). These parameters are: the non-dimensional failure driving force and the non-dimensional loading. This approach is now widely used for design and maintenance because it provides the safety factor associated with defect size, material fracture toughness, and loading. For the prediction of failure emanating from the notch, local and global stress criteria and a global energy criterion are used [6].

A local stress criterion such as VM is now widely applied for assessing a failure emanating from the notch. It is based on an accurate description of stress distribution in a closed volume near the notch tip. It incorporates two local parameters: the first – the effective stress and the second – the characteristic length. New trends incorporate the third parameter like a constraint, for example [7]. The local stress criterion was firstly suggested by Neuber in 1937 [3].

For the characteristic length, one distinguishes:

- a characteristic size  $\rho_c$  approximately equal to half the notch radius;
- a characteristic distance  $X_c$  connected to material microstructure;
- a critical distance  $d_0$  associated with the plastic zone and intrinsic of the material;

- an effective distance  $X_{\text{eff}}$  as a particular abscissa of stress distribution.

The choice of the characteristic length is based on the following considerations:

- the fracture process zone incorporates the maximum stress according to the concept “fracture process zone equal to the highest stressed region”;
- this length depends on the notch geometry, loading mode, constraint, etc.

A very small characteristic length is obtained for the brittle material. For the ductile material, the concept of the high-stress region cannot be applied to define a characteristic length or a critical distance. In the first case, the high stressed region is too small, in the second case – too large. The concept of the effective distance sensitive to constraint satisfies this condition. Consequently, the local fracture stress is also sensitive to the constraint.

Effective stress is defined as an average stress over a characteristic length. It was considered by Neuber [3] as a function of the notch radius. Novozhilov [4] and Sewe-

ryn [7] considered the mean normal stress as a failure criterion. Failure is triggered when the average stress equals the failure stress as a material value and is denoted by  $\sigma_c^*$ . In the line method [8], the average stress is considered along the effective distance  $X_{\text{eff}}$  or the critical distance  $d_0$  according to the authors or the characteristic distance  $X_c$ , according to the materials.

The fracture criterion (when using the effective distance  $X_{\text{eff}}$ ) can be written in the following generalized form including the mixed-mode fracture:

$$\frac{1}{X_{\text{eff}}} \max_{-\pi < \theta \leq \pi} \int_0^{X_{\text{eff}}} \sigma_{\theta\theta(r)} dr = \sigma_c^*, \quad (1)$$

Pluvinage [2] proposed averaging the stress distribution over the entire process volume  $V_{\text{eff}}$ . Then, the fracture criterion has the following form:

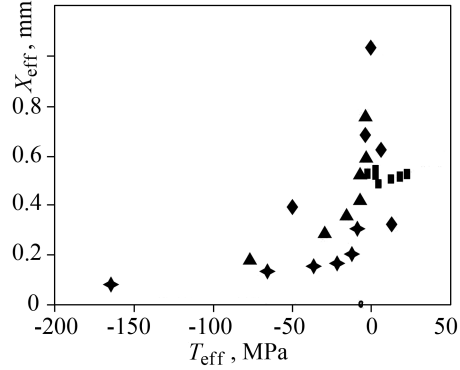
$$\frac{1}{V_{\text{eff}}} \iiint_{\Omega} \sigma_{yy}(x, y, z) \varphi(x, y, z) dV = \sigma_c^*, \quad (2)$$

where  $V_{\text{eff}}$  is the fracture process volume;  $\sigma_{yy}(x, y, z)$  are relative stress gradient and opening stress or maximum principal stress at the notch tip, respectively and  $\varphi(x, y, z)$  is a weight function.

If the line method is used, the size of the fracture process volume reduces the effective distance  $X_{\text{eff}}$ , which is obtained by the stress distribution analysis. Here, the high stressed region is limited at an inflexion point on the stress distribution curve that can be easily detected by a graphical or a numerical method associated with relative stress gradient  $\chi$ .

Effective distance is associated with the stress distribution which is sensitive to the constraint. Consequently, the effective distance is also sensitive to constraint as can be seen in Fig. 2. Several parameters were used to describe it: the constraint parameter  $L$  [9], the stress triaxiality [10], the  $Q$ -parameter [11] and  $T$ -stress [12]. Fig. 2 indicates a strong dependence of the effective distance on the constraint ( $T$ -stress).

Fig. 2. Evolution of the effective distance ( $X_{\text{eff}}$ ) versus effective  $T$ -stress ( $T_{\text{eff}}$ ) for the X52 pipe steel. Values obtained from four specimen types (◆ – compact tension (CT), ▲ – single-edge notched tension (SENT), ■ – double cantilever beam (DCB) and ◆ – rectangular tension (RT)).



Modification of lateral contraction owing to diminution of Poisson's effect can be represented by the  $T$ -stress which is one of the characteristics of the stress distribution at the crack or the notch tip. It was used as a constraint parameter. The following solution characterises the elastic stress fields in the region surrounding the notch tip [13]:

$$\sigma_{ij} = \frac{K_I}{\sqrt{2\pi r}} f_{ij}(\theta) + T\delta_{xi}\delta_{xj} + A_3\sqrt{2\pi r} + O(r), \quad (3)$$

where  $f_{ij}(\theta)$  is the angular function,  $\delta_{ij}$  is the symbol of Kronecker's determinant,  $K_I$  is the stress intensity factor (SIF) in the polar coordinate system  $(r, \theta)$ . The second term is the  $T$ -stress, constant stress acting parallel to the crack line in the direction  $xx$  of the

crack extension with a magnitude proportional to the gross stress. The  $T$ -stress may be tensile or compressive stress. The stress difference method is proposed by Yang et al. [14] to determine the  $T$ -stress.

In order to join the classical fracture mechanics and the concept of the SIF, the NSIF,  $K_\rho$ , can be defined as follow:

$$K_\rho = \sigma_{\text{eff}} (\pi X_{\text{eff}})^\alpha \sim \sigma_{\text{eff}} \sqrt{\pi X_{\text{eff}}} . \quad (4)$$

At failure

$$K_{\rho,c} = \sigma_{\text{eff},c} (\pi X_{\text{eff},c})^\alpha \sim \sigma_{\text{eff},c} \sqrt{\pi X_{\text{eff},c}} , \quad (5)$$

where  $X_{\text{eff},c}$  and  $\sigma_{\text{eff},c}$  are the critical values of the effective distance and the effective stress,  $\alpha$  is the governing parameter for local stress distribution. For an ideal notch ( $\rho = 0$ ),  $\alpha$  depends on notch angle  $\psi$ . According to Williams [13]:

$$\alpha(\psi) = 0.5 - 0.089 \left( \frac{\psi}{\pi} \right) + 0.442 \left( \frac{\psi}{\pi} \right)^2 - 0.853 \left( \frac{\psi}{\pi} \right)^3 . \quad (6)$$

For a crack ( $\rho = 0, \psi = 0$ )  $\alpha = 0.5$  and SIF the units have dimensions  $\text{MPa}\sqrt{\text{m}}$ . For a real notch ( $\rho \neq 0, \psi \neq 0$ )  $\alpha < 0.5$  and for the NSIF the units are  $\text{MPa}\cdot\text{m}^\alpha$ ! These strange units introduce a transferability problem if the notch fracture toughness is measured in the specimen with a notch angle different than that of the notch-like defect in the structure to assess.

**On notch fracture toughness.** For the failure emanating from a notch, the following criteria can be used as a critical event:

$$K_\rho = K_{\rho,c} \quad \text{and} \quad J_\rho = J_{\rho,c} , \quad (7)$$

The critical NSIF,  $K_{\rho,c}$  ( $\text{MPa}\cdot\text{m}^\alpha$ ) and critical notch  $J$ -integral,  $J_{\rho,c}$  are the parameters of material fracture toughness. These parameters are sensitive to the notch radius as can be seen in Fig. 3 and 4, where the notch fracture toughness of Al-Zn-Mg-Cu aluminium alloy was measured on SENT tensile specimens [15] and XC38 steel measured on TPB specimens [16] with different notch radius in the range 0...2 mm.

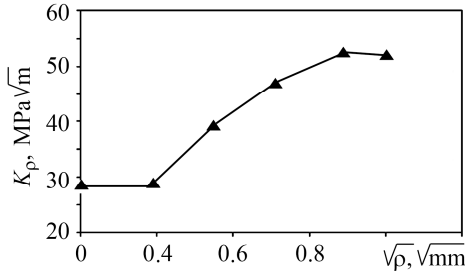


Fig. 3.

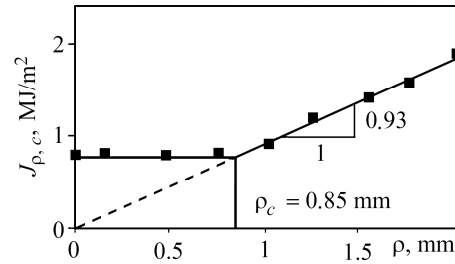


Fig. 4.

Fig. 3. Notch fracture toughness,  $K_\rho$ , of Al-Zn-Mg-Cu aluminium alloy measured on three point bend (TPB) specimens with different notch radius in the range 0...2 mm [15].

Fig. 4. Notch fracture toughness,  $J_{\rho,c}$ , of XC38 steel measured on TPB specimens with different notch radius in the range 0...2 mm [16].

It can be noted that fracture toughness increases with the notch radius beyond a critical notch radius,  $\rho_c$ , and is expressed by the following equation

$$K_{\rho,c} = K_{Ic} + \lambda\sqrt{\rho} \quad \text{for } \rho > \rho_c, \quad K_{\rho,c} = K_{Ic} \quad \text{for } \rho \leq \rho_c . \quad (8)$$

$$J_{\rho,c} = J_{Ic} + \beta\rho \quad \text{for } \rho > \rho_c, \quad J_{\rho,c} = J_{Ic} \quad \text{for } \rho \leq \rho_c . \quad (9)$$

Parameters  $\lambda$  and  $\beta$  are the notch fracture toughness sensitivity. The increase of the notch fracture toughness with a notch radius is explained by an extra plastic work in the notch plastic zone. For the notch radius  $\rho \leq \rho_c$  the notch plastic zone has a size less than the effective distance.  $K_{\rho,c}$  or  $J_{\rho,c}$  are governed by the effective distance, for  $\rho > \rho_c$  – by the notch plastic zone.

Hadj Meliani et al. [17] also pointed out the constraint effect on the notch fracture toughness  $K_{\rho,c}$ , the critical constraint being described by the critical effective  $T$ -stress,  $T_{\text{eff},c}$ . The material used in this study is the API X52 steel.

Specimens of four types, namely CT, DCB, SENT, and RT, were extracted from a steel pipe of a diameter of 610 mm. The specimens have a notch with an angle  $\psi = 0$ , a notch radius  $\rho = 0.25$  mm and an  $a/W$  ratio in the range 0.3...0.6. The stress distribution used was computed by the finite element method at a load level corresponding to the fracture load. The critical effective  $T$ -stress,  $T_{\text{eff},c}$  was determined according to VM. It can be noted in Fig. 5 that the notch fracture toughness decreases linearly with constraint according to:

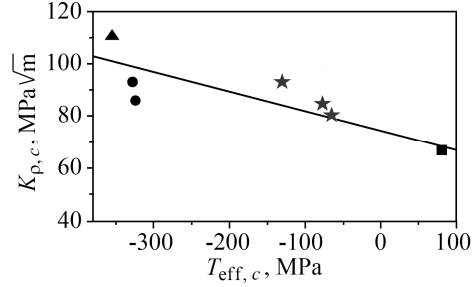


Fig. 5.  $K_{\rho,c}-T_{\text{eff},c}$  material failure master curve (MFMC) of low-carbon steel [17]: (★ – RT, ■ – DCB, ● – CT, ▲ – SENT).

$$K_{\rho,c} = aT_{\text{eff},c} + K_{\rho,c}^0, \quad (10)$$

where  $K_{\rho,c}^0$  is the fracture toughness corresponding to  $T_{\text{eff},c} = 0$  and considered as a reference;  $a = -0.069$  and  $K_{\rho,c}^0 = 77.3 \text{ MPa}\sqrt{\text{m}}$  for the API X52 pipe steel [17].

**On notch-like defect assessment.** The NFAD [18] methodology replaces the 3-fracture mechanics parameter relationship (fracture toughness, defect size and loading) by a two-parameter one in order to have a plane representation, where non-dimensional crack driving force and non-dimensional applied stress are the coordinates.

The applied non-dimensional fracture driving force is defined as a ratio of the applied NSIF  $K_{\rho,ap}$  and the notch fracture toughness of the material  $K_{\rho,c}$ .

$$k_r^* = K_{\rho,ap} / K_{\rho,c}. \quad (11)$$

The non-dimensional load is described as a ratio of the gross stress,  $\sigma_g$ , and flow stress chosen as yield stress,  $\sigma_y$ , ultimate stress,  $\sigma_{ul}$ , or classical flow stress  $\sigma_0 = (\sigma_y + \sigma_{ul}) / 2$

$$L_r = \sigma_g / \sigma_0. \quad (12)$$

The NFAD exhibits a failure curve as the critical non-dimensional crack driving force  $k_{r,c}$  versus the critical non-dimensional stress or loading parameter  $L_{r,c}$ . This curve  $k_{r,c} = f(L_{r,c})$  is the same as that used for the classical FAD. Fracture is determined by a high-stress triaxiality level. Such conditions ensure conservative conditions.

Plane strain conditions ahead of the crack tip lead to stress distribution with high constraint. Small thickness, blunt defect or tensile loading are generally encountered in real structures. Therefore, the constraint is reduced and local fracture toughness increases. To reduce conservatism, the NFAD is preferred for a notch-like defect. The failure assessment curve  $k_{r,c} = f(L_{r,c})$  delineates a fracture design curve according to the available codes, e.g. SINTAP [19].

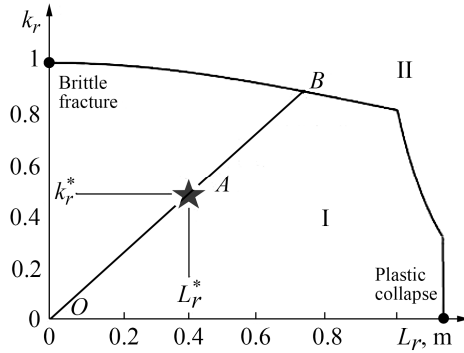


Fig. 6. Typical FAD (failure curve SINTAP level 1) that indicates safe (I) and failure zones (II), assessment point A and safety factor ( $f_s = OB/OA$ ) [19].

According to codes and safety factor consideration, the assessment point is positioned within the acceptable zone of the NFAD and the structure fulfils the required conditions for practical engineering applications. It is seen that fracture toughness is sensitive to the constraint. It increases when constraint decreases. This is the case when the defect promoting fracture is notch-like instead of crack-like. Therefore, again in order to reduce conservatism, the non-dimensional parameter  $k_r$  takes into account constraint.

Here, we assume that the constraint  $T$  is proportional to loading. This assumption is true for elastic behaviour but can be extended if a fracture occurs with little plasticity. The non-dimensional loading parameter  $L_r$  is described as a ratio of the applied load to the limit load  $p_L$ :

$$L_r = p/p_L. \quad (13)$$

The non-dimensional constraint  $T/\sigma_y$  is proportional to the loading parameter as:

$$T/\sigma_y = \beta_T L_r. \quad (14)$$

$\beta_T$  is the coefficient of proportionality and is obtained for different levels of loading represented by the non-dimensional loading parameter  $L_r$  assuming the elastic behaviour until cut for  $L_{r, \max} = 1.2$ .

For example, a pipe (Fig. 7a) made from API 5L X52 steel of yield stress  $\sigma_y = 465$  MPa and ultimate stress  $\sigma_{ul} = 528$  MPa is subjected to internal pressure. Pipe diameter is  $D = 610$  mm and pipe thickness  $t = 11$  mm. This pipe exhibits a surface notch of depth  $a = t/2$  and aspect ratio  $a/c = 0.2$ ,  $c$  is a half-notch length. The pipe limit pressure  $p_L = 20.1$  MPa. The effective  $T$ -stress,  $T_{\text{eff}}$ , is computed assuming elastic behaviour at any  $L_r$  values. The effective  $T$ -stress is defined as the corresponding value in the  $T$ -stress distribution equal to the effective distance,  $X_{\text{eff}}$ , given by VM [5]. This procedure is needed because the  $T$ -stress is not constant over the ligament.

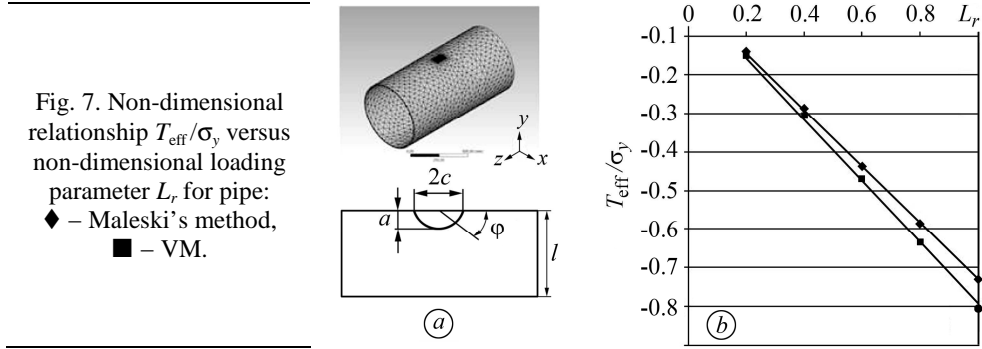
Maleski et al. [20] obtained the effective  $T$ -stress ( $T_{\text{eff}}$ ) by linear extrapolation of the origin of the  $T$  distribution. A comparison of the two methods is given in Fig. 7b.

The effective  $T$ -stress normalised by the yield stress versus the non-dimensional parameter  $L_r$  is presented in Fig. 7b. The relationship  $T_{\text{eff}}/\sigma_y = f(L_r)$  is linear with a constant slope  $\beta_T$ . The values of  $\beta_T$  are respectively  $\beta_T = 0.731$  for Maleski's method and  $\beta_T = 0.793$  for the VM. This latter value is chosen for reasons of being conservative.

The MFMC for API X52 pipe steel is described by Eq. (3), which can be rewritten as Eq. (8):

$$K_{\rho, c} = K_{\rho, c}^0 [1 + \alpha'(-\beta_T L_r, c)]. \quad (15)$$

Typical FAD indicating safe and failure zones, assessment points, and the safety factor is presented in Fig. 6. Coordinates  $k_r^*$  and  $L_r^*$  highlight the assessment point A of a component. If this point is inside the area delimited by the failure assessment curve, the structure is safe. If the assessment point is situated outside, failure occurs. Parameter  $k_r$  and  $L_r$  are proportional to the applied load for a constant notch or crack length; the loading path is linear from the origin to point B, where the failure assessment curve is reached. The safety factor  $f_s$  is defined by a ratio of  $OB$  to  $OA$ .



Parameter  $\alpha'$  depends on the constant  $\alpha$ , yield stress,  $\sigma_y$ , and reference fracture toughness,  $K_{\rho,c}^0$ .

By the introduction of the reference notch fracture toughness,  $K_{\rho,c}^0$ , in the definition of the non-dimensional  $k_r$  parameter, we assume that the reference failure assessment equation provided by SINTAP [19] corresponds to critical  $T$ -stress  $T = 0$ :

$$K_{r,T=0} = K_{ap} / K_{\rho,c}^0 = f(L_r). \quad (16)$$

Failure assessment curve is related to fracture toughness data measured from the specimens with an unknown constraint value but probably close to  $T = 0$ . The failure assessment curve for any value of constraint  $T$  is given as:

$$k_{r,c} = f(L_r)[1 + \alpha(-\beta_T L_{r,c})]. \quad (17)$$

The failure assessment curve is then modified according to Eq. (16) and the provided  $T$ -stress. Fig. 8 demonstrates the difference between two assessment curves:  $f(L_r)_{\text{struct}}$  and the reference failure assessment curve  $f(L_r)_{T=0}$  (Fig. 8).

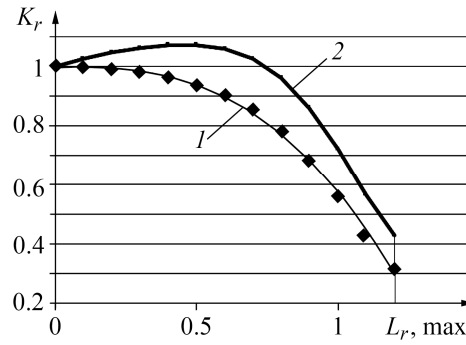


Fig. 8. Failure assessment curves [18]:  
1 –  $f(L_r)_{T=0}$ , 2 –  $f(L_r)_{\text{struct}}$ .

Three types of defect are considered

(Fig. 9): a central semi-spherical crack-like defect (SS) with depth  $d = t/2$ , a central semi-elliptical defect (SE) of length  $L$  ( $d = t/2$ ,  $d/L = 0.1$ ) and a central long blunt notch (LN) of notch radius  $r$  ( $d = t/2$ ,  $d/L = 0.1$ ,  $\rho = 0.15$  mm). The defect direction is longitudinal. The pipe has a diameter  $D = 219$  mm and a thickness  $t = 6.1$  mm. The service pressure is equal to 70 bars. Applied NSIF is reported in Table 1 and extracted from [21].

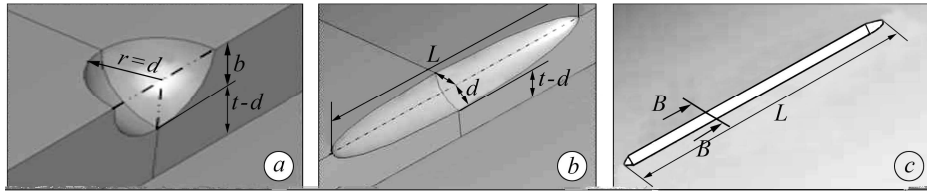


Fig. 9. Defect types: a –SS, b –SE, c –LN [21].

The reference fracture toughness is  $K_{\rho,c}^0 = 77.3 \text{ MPa}\sqrt{\text{m}}$  and the structure fracture toughness is  $K_{\rho,c}^{\text{struct}} = 100.4 \text{ MPa}\sqrt{\text{m}}$  corresponding to the critical effective constraint  $T_{\text{eff},c} = -335 \text{ MPa}$ .

**Table 1. Notch intensity factors in the longitudinal direction with 70 bars as the service pressure [21]**

Orientation of defect	Defect type	$K_\rho$ , MPa $\sqrt{\text{m}}$	$k_{r, \text{ref}}^*$	$k_{r, \text{struct}}^*$
Longitudinal direction	SS	12.4	0.16	0.12
	SE	14.5	0.18	0.14
	LN	19.7	0.25	0.19

The safety factor, defined as the relative distance from the assessment point to the intercept of the loading path with the failure assessment curve, was computed for the three defect types. The safety factor relative to the reference failure curve is called  $f_{s, T=0}$ , while that relative to the structure failure curve is  $f_{s, \text{struct}}$ . The results are reported in Table 2.

**Table 2. Safety factors associated with defects of different types (service pressure 70 bars)**

Defect type	$f_{s, T=0}$	$f_{s, \text{struct}}$	Difference, %
SS	3.16	3.44	9.1
SE	3.13	3.33	6.4
LN	3.04	3.01	3.7

**Discussion.** This paper presents the use of the NFM for a notch-like defect. Traditionally, any defect is considered as a crack-like defect as a conservative procedure and classical fracture mechanics (FM) are used for a defect assessment. Therefore, the similarity and difference between FM and NFM is an open question. Here we consider three kinds of notches: a crack ( $\rho = 0$ ,  $\psi = 0$ ), a notch with infinite acuity ( $\rho = 0$ ,  $\psi \neq 0$ ) and a simple notch ( $\rho \neq 0$ ,  $\psi \neq 0$ ). Therefore, a crack is a special case of a notch.

A crack is mathematically a plane cut. The zero notch radius infinite acuity  $1/r$  leads to a  $r^{-0.5}$  stress singularity with the distance  $r$  to the crack tip. The stress distribution is characterized by the SIF  $K$  related to opening stress,  $\sigma_{yy}$ , by:

$$K = \sqrt{2\pi} \lim_{r \rightarrow 0} \sigma_{yy} \sqrt{r} . \quad (18)$$

In the case of the crack, a unit of the SIF is MPa $\sqrt{\text{m}}$  that is not really a simple unit. For an ideal notch the SIF  $K^*$  is given by ( $\rho = 0$ ,  $\psi \neq 0$ ):

$$K^* = 2\pi^\alpha \lim_{r \rightarrow 0} \sigma_{yy} r^\alpha . \quad (19)$$

The singularity exponent  $\alpha$  is given by the Williams solution [13] in Eq. (6). For a simple notch the NSIF, due to the fact that the maximum stress is finite (no singularity), is expressed by:

$$K_\rho = 2\pi^\alpha \sigma_{yy} r^\alpha , \quad r \geq X_{\text{eff}} . \quad (20)$$

Units are again MPa $\cdot\text{m}^\alpha$ . Therefore the use of the SIF concept is complicated due to the unit problem. This difficulty can be solved by using non-dimensional opening stress at effective distance,  $\tilde{\sigma}_{\text{eff}}$ , (critical distance for a crack or an ideal notch):

$$\tilde{\sigma}_{\text{eff}} = \frac{K}{\sqrt{r}} \quad \text{or} \quad \frac{K^*}{r^\alpha} \quad \text{or} \quad \frac{K_\rho}{r^\alpha} . \quad (21)$$

It is simpler to use directly the effective stress given by VM [5]. The use of the NFM with the concept of a notch-like defect is introduced in order to reduce the con-



servatism of using classical fracture mechanics with the concept of a crack-like defect. Two approaches are compared with the two following defects in a pipe subjected to internal pressure: a surface long blunt notch of a radius  $\rho$  ( $d = t/2$ ,  $d/L = 0.1$ ,  $\rho = 0.15$  mm) and a semi-elliptical surface crack of a length  $2c = 5t$ . The defect direction is longitudinal. The pipe has a diameter  $D = 219$  mm and a thickness  $t = 6.1$  mm. The service pressure is equal to 70 bars. Depth of the defect (a crack or a notch) is  $a = t/2$ , the crack or the notch lengths are identical. Pipe steel is API 5L X52 with a reference fracture toughness  $K_{\rho, c}^0 = 77.3 \text{ MPa}\sqrt{\text{m}}$ .

The SIF for a crack and the NSIF for a long notch are computed by FEM. The results are presented in Table 3. The safety factor is computed according to the FAD method.

**Table 3. The SIF for a crack and the NSIF for a long notch in the FAD coordinates and associated safety factor**

Defect type	SIF or NSIF, $\text{MPa}\sqrt{\text{m}}$	$k_r$	$L_r$	$f_{s, T}$
Crack	30.8	0.30	0.26	2.55
Long notch	22.87	0.40	0.26	3.03

It can be noted that the crack-like defect leads to over-conservatism (lower safety factor). The difference between the crack-like defect and NFM is about 15.8%.

### CONCLUSION

The notch-like defect assessment cannot be done with over-conservatism using the classical fracture mechanics (mechanics of cracks). In this case, the use of the NFM is preferable. This can be done using either local effective stress, notch energy integral or NSIF. The use of the NSIF ensures a continuous approach with classical fracture mechanics considering that a crack is a special case of a notch. However, the NSIF units are complex and generate transferability problem when constraint and notch geometry are different in the structure and specimens used for the notch fracture toughness determination. Notch fracture toughness is sensitive to the notch radius and is equal to the crack fracture toughness for a notch radius less than a critical one. For large radii, notch fracture toughness incorporates notch plastic work which is, in this case, greater than the fracture process zone. This constraint in a modified NFAD is also taken into account. Using this tool, the reduction of the conservatism applied to the safety factor is in the range 10...20%. This is mainly applied for oil and gas pipes for which defects, caused by external interferences represent more than 50% of a defect provoking pipe failure.

*РЕЗЮМЕ.* Оцінено дефекти типу надрізу без використання класичних підходів механіки руйнування (механіки тріщин). Застосовано поняття коефіцієнта інтенсивності напружень або  $J_{\rho}$ -інтеграла для вирізу зі заданим радіусом заокруглення. При цьому локальне напруження біля надрізу розраховано об'ємним методом, який встановлює певне ефективне напруження із урахуванням геометрії надрізу та ефекту обмеження напружень біля його вершини. Ці чинники взято до уваги під час визначення в'язкості руйнування та побудови модифікованих діаграм оцінювання руйнування біля надрізів.

**Ключові слова:** надріз, механіка руйнування, діаграма оцінки руйнування.

*РЕЗЮМЕ.* Оценены дефекты типа надреза без использования классических подходов механики разрушения (механики трещин). Применено понятие коэффициента интенсивности напряжений или  $J_{\rho}$ -интеграла для выреза с заданным радиусом закругления. При этом локальное напряжение возле надреза рассчитано объемным методом, который устанавливает определенное эффективное напряжение с учетом геометрии надреза и эффекта ограничения напряжений у его вершины. Эти факторы приняты во внимание при

определении вязкости разрушения и построении модифицированных диаграмм оценки разрушения возле надрезов.

**Ключевые слова:** надрез, механика разрушения, диаграмма оценки разрушения.

1. 7<sup>th</sup> Report of European Gas Pipeline Incident Data Group, 1970–2007: Gas pipeline Incidents. – EGIG, Netherlands, 2008. – 33 p.
2. Pluvinage G. Notch Effects in Fatigue and Fracture // Notch Effects in Fatigue and Fracture / Ed. G. Pluvinage, M. Gjonaj. NATO Science Series (Series II: Mathematics, Physics and Chemistry). – Dordrecht: Kluwer, 2001. – 11. – P. 1–22.
3. Neuber H. Kerbspannungslehre. – Berlin: Springer, 1937. – 326 p.
4. Novozhilov V. V. On a necessary and sufficient criterion for brittle strength // J. of App. Math. and Mech. – 1969. – 33, № 2. – P. 212–222.
5. Fracture toughness of high-strength steel using the notch stress intensity factor and volumetric approach / H. El Minor, A. Kifani, M. Louah, Z. Azari, G. Pluvinage // Structural Safety. – 2003. – 25, Is. 1. – P. 35–45.
6. Pluvinage G. Mécanique élastoplastique de la rupture – Critères d’amorçage. – Toulouse: Cepadues, 1989. – 512 p.
7. Seweryn A. Brittle fracture criterion for structures with sharp notches // Engng. Frac. Mech. – 1994. – 47, Is. 5. – P. 673–681.
8. Taylor D. Predicting the fracture strength of ceramic materials using the theory of critical distances // Engng. Frac. Mech. – 2004. – 71, Is. 16–17. – P. 2407–2416.
9. Mouwakeh M., Pluvinage G., and Masri S. Failure of water pipes containing surface cracks using limit analysis notions // Res. J. of Aleppo Univ. Engng. Sci. Series. – 2011. – 63. – P. 1–23.
10. Henry B. S. and Luxmore A. R. The stress triaxiality constraint and the Q-value as a ductile fracture parameter // Engng. Frac. Mech. – 1997. – 57, Is. 4. – P. 375–390.
11. Ruggieri C., Gao X., and Dodds R. H. Transferability of elastic–plastic fracture toughness using the Weibull stress approach: Significance of parameter calibration // Engng. Frac. Mech. – 2000. – 67, Is. 2. – P. 101–117.
12. Larsson S. G. and Carlsson A. J. Influence of non-singular stress terms and specimen geometry on small-scale yielding at crack tips in elastic-plastic materials // J. of Mech. and Phys. of Solids. – 1973. – 21, Is. 4. – P. 263–277.
13. Williams M. L. On the stress distribution at the base of stationary Crack // J. of App. Mech. – 1956. – 24, Is. 1. – P. 109–114.
14. Yang B. and Ravi-Chandar K. Evaluation of elastic T-stress by the stress difference method // Engng. Frac. Mech. – 1999. – 64, Is. 5. – P. 589–605.
15. Influence of notch radius and microstructure on the fracture behavior of Al–Zn–Mg–Cu alloys of different purity / M. Vratnica, G. Pluvinage, P. Jodin, Z. Cvijović, M. Rakin, Z. Burzić // Materials & Design. – 2010. – 31, Is. 4. – P. 1790–1798.
16. The effect of notch radius on fracture toughness  $J_{Ic}$  / O. Akourri, M. Louah, A. Kifani, G. Gilgert, G. Pluvinage // Engng. Frac. Mech. – 2000. – 65, Is. 4. – P. 491–505.
17. Meliani M. H., Matvienko Y. G., and Pluvinage G. Two-parameter fracture criterion ( $K_p, c - T_{ef, c}$ ) based on notch fracture mechanics // Int. J. Frac. – 2011. – 167, Is. 2. – P. 173–182.
18. Pluvinage G., Capelle J., and Schmidt C. Methods for assessing defects leading to gas pipe failure (Chapter 3) // Handbook of Materials Failure Analysis with Case Studies from the Oil and Gas Industry / Ed. A. S. H. Makhoul, M. Aliofkhaezrai. – Butterworth-Heinemann, 2016. – P. 55–89.
19. SINTAP: Structural Integrity Assessment Procedure. Final Report. EU-Project BE 95-1462. Brite Euram Programme. – Brussels, 1999.
20. Maleski M. J., Kirugulige M. S., and Tippur H. V. A Method for measuring mode I crack tip constraint under static and dynamic loading conditions // Experimental Mechanics. – 2004. – 44, Is. 5. – P. 522–532.
21. Adib-Ramezani H., Jeong J., and Pluvinage G. Structural integrity evaluation of X52 gas pipes subjected to external corrosion defects using the SINTAP procedure // Int. J. of Pressure Vessels and Piping. – 2006. – 83, Is. 6. – P. 420–432.

Received 21.08.2019